Real-time spectroscopic ellipsometry study of the growth of amorphous and microcrystalline silicon thin films prepared by alternating silicon deposition and hydrogen plasma treatment

N. Layadi,* P. Roca i Cabarrocas,† and B. Drévillon
Laboratoire de Physique des Interfaces et des Couches Minces (UPR 258 du CNRS), Ecole Polytechnique, 91128 Palaiseau, France

I. Solomon
Laboratoire de Physique de la Matière Condensée (URA 1254 du CNRS), Ecole Polytechnique, 91128 Palaiseau, France
(Received 17 February 1995; revised manuscript received 17 April 1995)

The growth of amorphous and microcrystalline silicon (μc-Si) films prepared by alternating the deposition of hydrogenated amorphous silicon (a-Si:H) and hydrogen plasma exposure is studied by *in situ* spectroscopic ellipsometry. The deposition and etching sequences are clearly identified in the real-time ellipsometric trajectories. Insights into the growth of amorphous and microcrystalline silicon materials are obtained from a detailed study of the effects of varying the deposition and hydrogen plasma treatment times as well as the thickness dependence of the film composition. Indeed, we have found that the composition of amorphous and microcrystalline films slowly changes with the increasing film thickness. However, while a-Si:H films become porous and rough with the increasing number of cycles, μc-Si films become denser and their crystalline volume fraction increases. During growth, the transition from a-Si:H to μc-Si deposition occurs through an intermediate highly porous a-Si:H phase. We suggest that this porous phase is a key element in μc-Si nucleation, while both selective etching and chemical annealing have to be considered in the growth of the crystallites. Our results show that it is possible to increase the volume fraction of the crystalline phase by reducing the deposition time within one cycle or by increasing the hydrogen plasma treatment time.

I. INTRODUCTION

Microcrystalline silicon thin films (μc-Si) present interesting properties for device applications. In particular, as compared to a-Si:H material, μc-Si exhibits unique properties like higher doping efficiency and better electrical conductivity and carrier mobility, together with a lower optical absorption.[1] Therefore, many studies have been devoted to an analysis of the growth mechanisms of μc-Si to better control and further improve its properties. While the transition from amorphous to microcrystalline silicon has been revealed by *in situ* Raman spectroscopy,[2] *in situ* ellipsometry has also been used extensively to provide a detailed description of the nucleation, growth, and structure of μc-Si.[3–5] Despite the large number of studies, the growth mechanisms and the role of hydrogen atoms on the formation of μc-Si are not fully understood.

In order to obtain more detailed information on the processes involved in μc-Si deposition, a-Si:H and μc-Si films have also been prepared by alternating the deposition of a few monolayers of a-Si:H and its exposure to a H_2 plasma (layer-by-layer technique).[6–8] By separating in time the deposition of a-Si:H from the H_2 plasma treatment sequence, one may expect a simpler plasma chemistry and therefore an easier identification of the influence of hydrogen atoms on the growth mechanisms.

Here we report an *in situ* spectroscopic ellipsometry analysis of the layer-by-layer (LBL) deposition of amorphous and microcrystalline silicon films at 250 °C on glass substrates. Insights into the growth mechanisms are given. In particular the influence of deposition and etching times on μc-Si deposition is presented.

II. EXPERIMENTAL DETAILS

A. Deposition and etching conditions

We use the layer-by-layer deposition technique in a capacitively coupled rf (13.56 MHz) glow discharge system. This technique consists of repeating a series of successive plasmas: deposition of a-Si:H during time T_{Si} and its exposure to a H_2 plasma during T_H (see Fig. 1). T_{r1} ($\approx$90 s) and T_{r2} ($\approx$40 s) are the dead times necessary to adjust the gas pressure before each deposition and etching sequence, respectively. The films were deposited on

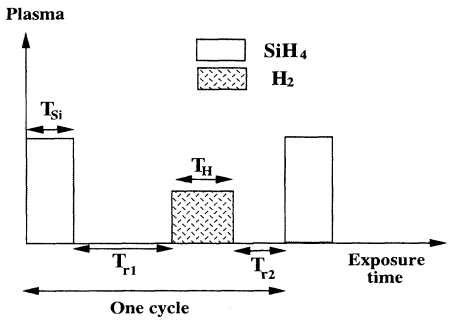

FIG. 1. Schematic diagram of the deposition of amorphous and microcrystalline silicon films by alternating sequences of silane and hydrogen plasmas during T_{Si} and T_H, respectively. T_{r1} (T_{r2}) represents the waiting time before each etching (deposition) of several monolayers after turning off the H_2 (SiH_4) plasma, (T_{r1}=90 s, T_{r2}=40 s). This procedure is repeated N times to obtain $\approx$1000-Å-thick films.

Corning 7059 glass substrates at 250 °C. The influence of the substrate on the μc-Si formation is discussed elsewhere.[9] The deposition and etching conditions used in this study are summarized in Table I. We emphasize that these deposition conditions produce a-Si:H films with a low defect density at a deposition rate of 0.85 Å/s. If the times T_{Si} and T_H are very short, the LBL technique is equivalent to a commonly used dilution of silane in hydrogen. One may consider the LBL technique as a dilution in time rather than a dilution obtained by the mixing of gases.

The structure of the deposited materials (amorphous or crystalline) has been determined *in situ* by spectroscopic ellipsometry and verified, for some samples, by dark conductivity and Raman-scattering measurements.

B. Real-time spectroscopic ellipsometry

In situ spectroscopic ellipsometry is well adapted to study microcrystalline materials because it provides a direct identification of the crystallinity from the measurement of the dielectric function.[10,11] Spectroscopic ellipsometry measurements were taken at different stages of the layer-by-layer deposition to check for the nature (amorphous or microcrystalline) of the deposited films when T_H and T_{Si} were varied. In this way we can follow *in situ* and in real time the evolution of the films. The *in situ* ellipsometry technique and the computer-controlled gas handling system turned out to be essential for the deposition and analysis of a large number of reproducible layers. More details concerning the experimental setup and the UV-visible ellipsometer can be found elsewhere.[12,13]

We recall that ellipsometry measures the ratio

$$\rho=\frac{r_p}{r_s}=\tan(\Psi)\exp(i\Delta)\ , \tag{1}$$

where Ψ and Δ are the conventional ellipsometric angles. The subscripts p and s refer to the plane-wave electric-field components, respectively, parallel and perpendicular to the plane of incidence.[14]

The pseudodielectric function $\langle\varepsilon\rangle$ is obtained from the measurement of ρ:

$$\langle\varepsilon\rangle=\langle\varepsilon_1\rangle+i\langle\varepsilon_2\rangle$$
$$=\sin^2\phi_0+\left[\frac{1-\rho}{1+\rho}\right]^2\sin^2\phi_0\tan^2\phi_0\ , \tag{2}$$

TABLE I. Deposition and etching conditions used for the preparation of films by the layer-by-layer technique. The experimental conditions used for a-Si:H deposition produce device quality material at a deposition rate close to 0.85 Å/s.

	Deposition	Etching
RF power density (mW cm^{-2})	88	222
Flow rate of SiH_4 (sccm)	3,5	0
Flow rate of H_2 (sccm)	0	35
Pressure (mTorr)	100	240
Substrate temperature (°C)	250	250
Plasma exposure time (s)	T_{Si}	T_H

where ϕ_0 is the angle of incidence (76° in our experimental setup). For an opaque film, with a smooth surface, the pseudodielectric function $\langle\varepsilon\rangle$ is equal to the dielectric function ε.

Microcrystalline silicon films are usually described as a mixture of small crystallites embedded in an amorphous matrix, using a three-phase model: microcrystallites,[15] amorphous,[16] and voids. More precisely the Bruggeman effective-medium approximation (BEMA) (Ref. 17) is used to describe this kind of material. It allows the determination of the dielectric function ε_{eff} of the composite material as a function of the dielectric response of its constituents ε_i and their relative volume fraction f_i:

$$\sum_i f_i\frac{\varepsilon_i-\varepsilon_{eff}}{\varepsilon_i+2\varepsilon_{eff}}=0\ . \tag{3}$$

A more refined analysis should include shape and finite-size effects on the optical functions of the crystallites.[18] However, our purpose is to determine general trends, and these effects are considered of second order and out of the scope of this study.

III. RESULTS AND DISCUSSION

A. Steady state

In Fig. 2 we present the phase diagram of silicon films deposited on glass substrates at 250 °C by the LBL technique. The nature of the films was deduced from *in situ* ellipsometry measurements performed at different stages of deposition. This allowed us to check that the steady state was reached (typically for 100-nm-thick films). Depending on the thickness of the stacking layers (proportional to T_{Si}) and on the ratio $R=(T_H/T_{Si})$, the deposit-

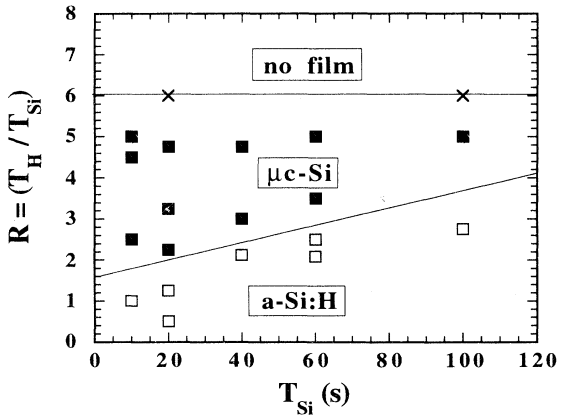

FIG. 2. Space of parameters for the growth of amorphous and microcrystalline silicon films deposited by the layer-by-layer technique on glass substrates at 250 °C. The deposition time T_{Si} and the ratio $R=T_H/T_{Si}$ are the main parameters which control the nature of the films. The lines between amorphous, microcrystalline, and no deposition conditions are provided as a guide to the eye. The no film region corresponds to values of R for which the a-Si:H film deposited during T_{Si} is fully removed by the hydrogen plasma of duration T_H. The experimental points represent the steady state ($\approx$1000-Å-thick films).

ed films are amorphous or microcrystalline. For high values of R no deposition is observed. For short exposure times to H_2 plasma (low values of R) the silicon films remain amorphous. A sufficient exposure time T_H is needed to produce the transition from a-Si:H to μc-Si deposition. This transition time increases as a function of T_{Si} (stacking layer thickness). Finally, if T_H is too long no film is deposited. This last trend can be considered as evidence of the etching effect induced by the hydrogen plasma. The transition from μc-Si deposition to no film growth is obtained for $R \geq 6$, i.e., at $R \approx 6$ the etching rate overtakes that of the deposition and there is no material deposited. The experimental results indicate that the borderline between μc-Si growth and no film occurs at a constant R. In contrast, the value of R at which the transition from a-Si:H to μc-Si growth occurs increases as T_{Si} increases (Fig. 2). It has to be pointed out that these boundary values of R are obtained with the experimental conditions given in Table I, and are not intrinsic ones but related to the balance between the deposition and etching rates.

In Fig. 3 we plot the average deposition rate of the films, deduced from the ratio between the film thickness and the deposition time, as a function of the hydrogen plasma exposure time T_H. The average deposition rate can be expressed as $\bar{v} = v_d - v_g(T_H/T_{Si})$ where v_d and v_g are the deposition and etching rates, respectively. It is clear from Fig. 3 that the average deposition rate decreases when the H_2 exposure time increases, independently of T_{Si}. The inset in Fig. 3 shows the effective layer thickness deposited per cycle, defined by $\bar{e}_p = v_d T_{Si} - v_g T_H$, as a function of hydrogen exposure time (for $T_{Si} = 20$ s). These data indicate that, with respect to the reference a-Si:H sample, μc-Si films are obtained when the macroscopic etching is about 30% of the film thickness per cycle; i.e., μc-Si is formed when there is a sufficient etching of the deposited material. However, under conditions corresponding to the boundary between the amorphous to microcrystalline silicon film growth (25 s $\leq T_H \leq$ 40 s, in Fig. 3), we remark that there is no discontinuity between a-Si:H and μc-Si deposition rate. This may explain some claims about etching not being important in μc-Si deposition.[6]

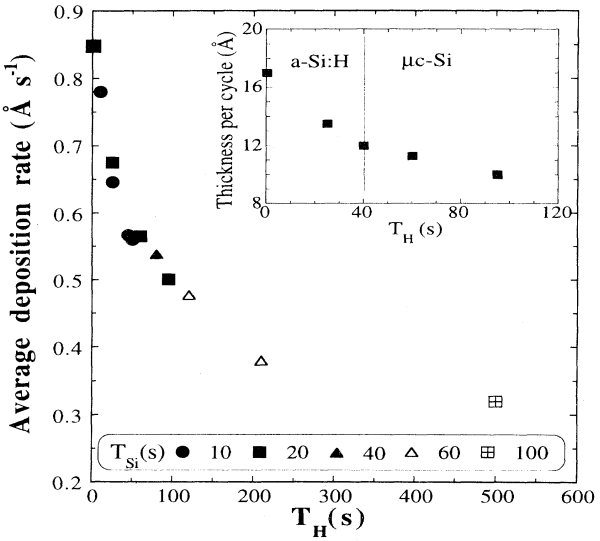

FIG. 3. Average deposition rate of materials deposited by the layer-by-layer technique plotted against T_H for different T_{Si}. The deposition rate was obtained by dividing the total thickness by the total deposition time. The average deposition rate decreases by increasing the H_2 exposure time independently on T_{Si}. The inset shows the deposited thickness per cycle as a function of T_H, for $T_{Si} = 20$ s. The transition from a-Si:H to μc-Si deposition is accompanied with a macroscopic etching of about 30%.

For a fixed T_{Si}, the average deposition rate and the deposited layer thickness per cycle should be proportional to T_H. However, the data presented in Fig. 3 do not show a linear dependence, suggesting that the growth and etching rates are not constant. This is well understood by the fact that the etching rate of a-Si:H is higher than that of crystalline silicon, and also that as T_H increases the crystalline fraction increases, resulting in a decrease of the etching rate.

B. Study of the transients

1. *Real-time study of deposition and etching*

Figure 4 displays the real-time evolution (at three probing wavelengths) of the ellipsometric angle Δ obtained during the deposition of μc-Si by the LBL technique with $T_{Si} = 20$ s and $T_H = 95$ s. In fact, Fig. 4 qualitatively describes the evolution in time of the film thickness during the layer-by-layer deposition. Indeed, in the case of thin films ($d_f \ll \lambda$), the variation of the phase Δ is proportional to the variation of the thickness of the sample.[19] The deposition and etching sequences are clearly identified by the real-time trajectories. We notice that there is no evolution during the plasma-off times, so that the properties of the films are independent of the dead times T_{r1} and T_{r2}. This is probably not the case at higher temperature because of hydrogen desorption and modification of the surface-hydrogen coverage.[20] In our study we varied only T_{Si} and T_H, the dead times being maintained constant.

2. *Layer-by-layer growth under amorphous silicon conditions*

Figure 5 shows the imaginary part of the pseudodielectric function $\langle \varepsilon_2 \rangle$ measured at different stages of the deposition of a-Si:H by the LBL technique at $T_{Si} = 20$ s and $T_H = 25$ s. Figure 5 reveals that more than 100 cycles (deposition and etching steps) have to be accumulated before reaching a steady state. Moreover, the overall decrease in amplitude of $\langle \varepsilon_2 \rangle$ with an increasing number of cycles suggests that the porosity of a-Si:H films increases as a function of the film thickness. This evolution has been found to be reproducible for the deposition of all a-Si:H films shown in Fig. 2, independently of the value of T_{Si}. Hence hydrogen etching leads to the formation of porous a-Si:H films, as already reported.[21]

In order to obtain more detailed information on the evolution of the film properties as a function of thickness,

the spectroscopic ellipsometry measurements presented in Fig. 5 have been simulated using BEMA and considering a model of two layers: the bulk and the surface roughness. Each layer is assumed to be a homogeneous mixture of an amorphous phase (volume fraction f_a), and voids ($1-f_a$). The results of such an analysis are presented in Fig. 6. We observe that the amorphous fraction in the bulk decreases down to 80% for a film thickness of 1450 Å. At the same time the thickness of the surface roughness increases and reaches 40 Å. At this thickness the amorphous fraction on the surface is 60%. The results of Figs. 5 and 6 indicate that amorphous silicon films prepared by the layer-by-layer technique are not dense. On the other hand, it has been suggested that the layer-by-layer technique could be used to prepare more rigid silicon networks.[22]

More generally, the analysis of the films presented in Fig. 2 indicates that the increase in porosity is enhanced, especially under the critical conditions corresponding to the boundary between the amorphous and microcrystalline silicon deposition: the deposited *a*-Si:H material goes through a highly porous and defective amorphous phase before reaching the crystallization threshold. As will be discussed below, this point is essential for understanding the nucleation mechanisms of μc-Si.

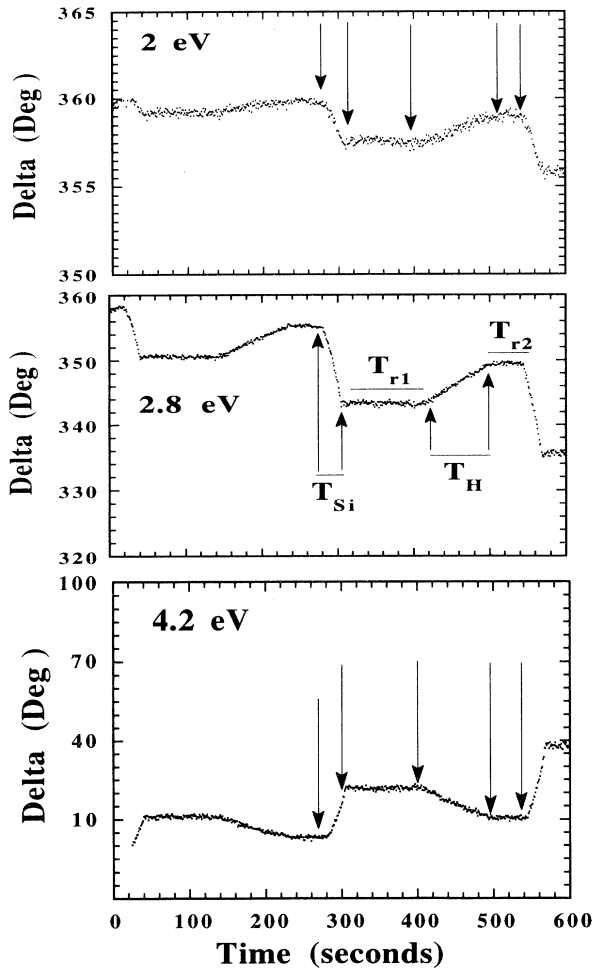

FIG. 4. Real-time trajectories of the ellipsometric angle Δ with time, at three photon energies, during the deposition of microcrystalline silicon film by the layer-by-layer technique at $T_{Si}=20$ s and $T_H=95$ s, on glass substrate, at 250 °C. Note that there is no modification of the optical properties during the waiting times ($T_{r1}=90$ s and $T_{r2}=40$ s).

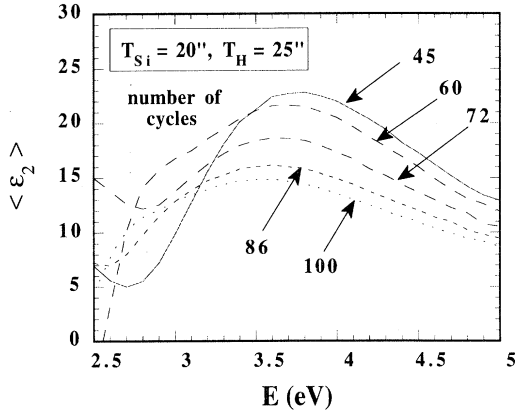

FIG. 5. Evolution of the imaginary part of the pseudodielectric function of an *a*-Si:H film deposited by the layer-by-layer technique with $T_{Si}=20$ s and $T_H=25$ s.

3. *Layer-by-layer nucleation and growth of films under microcrystalline conditions*

Figure 7 shows the time evolution of $\langle \varepsilon_2 \rangle$ for a μc-Si film deposited at $T_{Si}=20$ s and $T_H=95$ s. As in the case of *a*-Si:H deposition (Fig. 5), up to 100 cycles are needed to reach the steady state. In contrast to the deposition under amorphous conditions there is an *increase* of $\langle \varepsilon_2 \rangle$ with the number of cycles, indicating that the film becomes denser. We note that this evolution of $\langle \varepsilon_2 \rangle$ is opposite to that observed during deposition of μc-Si films from the decomposition of highly diluted silane in hydrogen mixtures,[4] indicating that the LBL technique is

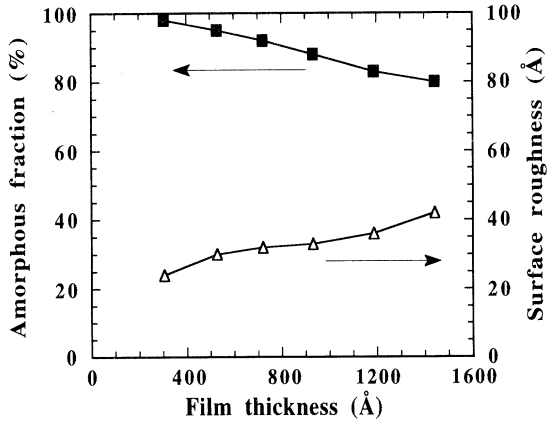

FIG. 6. Evolution of the bulk composition and the thickness of the surface roughness during the deposition of *a*-Si:H films by the layer-by-layer technique ($T_{Si}=20$ s, $T_H=25$ s). These results are deduced from the fitting of spectra of Fig. 5 using BEMA analysis.

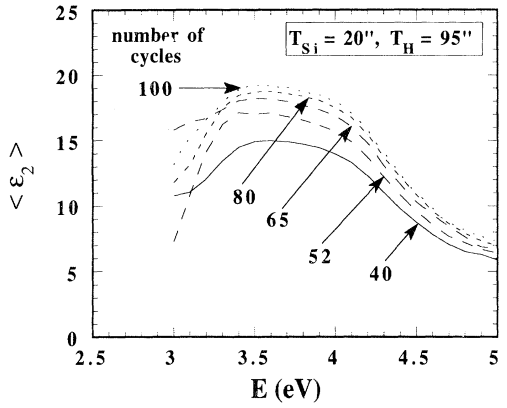

FIG. 7. Evolution of the imaginary part of the pseudodielectric function of a μc-Si film deposited by the layer-by-layer technique with $T_{Si}=20$ s and $T_H=95$ s.

better suited than conventional hydrogen dilution for the deposition of dense μc-Si films. The spectroscopic ellipsometry measurement presented in Fig. 7 have been simulated using BEMA and considering, as in the case of a-Si:H deposition, a model with two layers: the bulk and the surface roughness. Each layer is assumed to be a homogeneous mixture of three phases: amorphous (volume fraction f_a), crystal (f_c), and voids ($f_v=1-f_a-f_c$).

As an example of fitting we present, in Fig. 8, the experimental and fitted values of the real and imaginary parts of the pseudodielectric function for a μc-Si film obtained after 100 cycles of alternating deposition ($T_{Si}=20$ s) and hydrogen plasma exposure ($T_H=95$ s). As shown in the figure, the film can be described by a 1030-Å-thick bulk layer containing 22% amorphous silicon, 64% crystallites, and 14% voids, plus a 60-Å-thick surface layer containing 21% amorphous silicon, 37% microcrystallites, and 42% voids. We emphasize that the bulk composition is considered to be homogeneous and that the crystalline fraction in the bulk is much higher than in the surface.

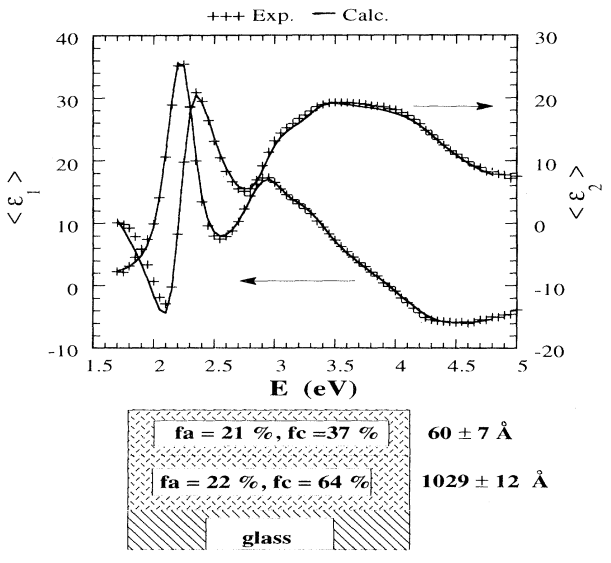

FIG. 8. Pseudodielectric functions $\langle \varepsilon_1 \rangle$ and $\langle \varepsilon_2 \rangle$ experimentally determined (+++) for the μc-Si film obtained after 100 cycles with $T_{Si}=20$ s and $T_H=95$ s. Also plotted is the calculated result (——) based on the structure schematically shown in the bottom of the figure. Note the good quality of the fit.

Figure 9 shows the evolution of the surface and bulk composition deduced from BEMA analysis of the spectroscopic data presented in Fig. 7. The thickness of the surface layer (not shown) increases up to 60 Å for a film thickness of 400 Å, and remains constant thereafter. The composition of this surface layer slowly changes, and the steady state is only attained for a film thickness of about 1000 Å. Therefore, up to 400 Å, both the thickness of the surface layer and its composition change. Above this value the thickness of the surface layer remains constant while its composition continues to evolve.

The thickness dependence of the bulk composition (Fig. 9) reveals the following.

(i) The film starts to grow amorphous, up to a thickness of about 100 Å and afterward becomes microcrystalline. We stress that according to our model (homogeneous composition) the film crystallizes down to the interface with the substrate, in agreement with *in situ* Raman-scattering measurements.[2] The amorphous layer observed during the initial growth has been attributed to some chemical reactions occurring during the exposure of the glass substrate to the silane or hydrogen plasmas.[23] However, this chemical interface, which favors the amor-

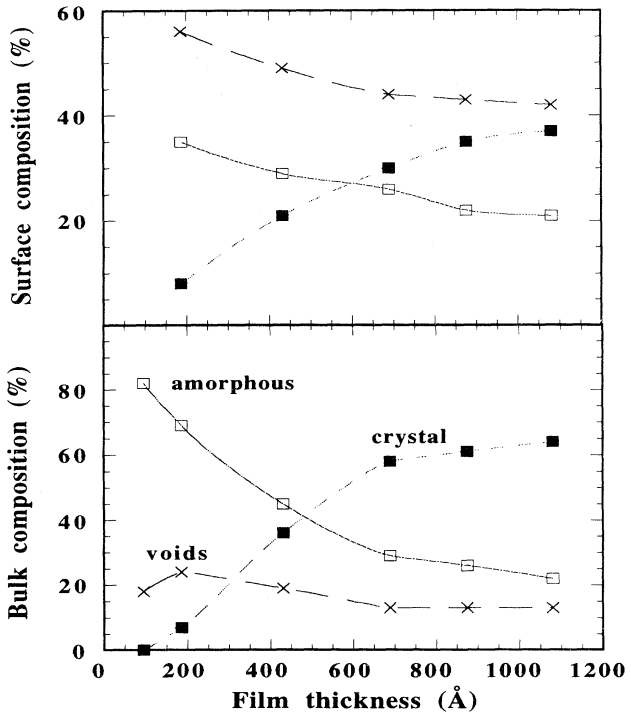

FIG. 9. Evolution of composition of the surface and bulk in a μc-Si film deposited by the layer-by-layer technique with $T_{Si}=20$ s, $T_H=95$ s. These results are deduced from BEMA analysis and fitting of spectra shown in Fig. 7.

phous rather than the crystal formation during the early stage of deposition, does not prevent the ulterior crystallization of the film down to the interface with the glass substrate.

(ii) The transition from a-Si:H to μc-Si growth is accompanied by an increase in the bulk porosity, up to 24% for a film thickness of 200 Å, and is reduced down to 13% during further film growth. Therefore we observe the same kind of behavior in both steady-state (Fig. 4) and transient regimes, i.e., an increase of the film porosity for films which are at the boundary between a-Si:H and μc-Si deposition.

(iii) During growth there is an increase of the volume fraction of crystallites and a decrease of the volume fraction of the amorphous phase, indicating that the increase of the crystalline phase in the bulk occurs due to the crystallization of the amorphous phase.

(iv) The bulk is much more crystallized than the surface. This difference in structure between the surface and the bulk has also been observed by Raman spectroscopy.[24] These results indicate that the etching is not the only process responsible for μc-Si growth, and suggest that the diffusion of atomic hydrogen is probably responsible for the increase of the crystalline phase in the bulk and the development of the crystallites. This mechanism, which has been proposed for film thicknesses up to 4 nm,[25] extends under our conditions over some tens of nanometers. Indeed, some recent reports indicate that atomic hydrogen can diffuse through long distances before being trapped.[26]

4. *Effects of deposition and etching times on μc-Si growth*

Figure 10 shows the effect of varying T_H or T_{Si} on the evolution of the crystalline fraction as a function of the thickness. For a fixed deposition time ($T_{Si}=20$ s) and two values of the ratio $R=T_H/T_{Si}$, we observe that (i) there is an incubation period (thickness ≈ 100 Å) during which the film is amorphous, and becomes microcrystalline for thicknesses $>$ 100 Å; (ii) the crystalline fraction increases with film thickness; and (iii) the film prepared at $R=4.75$ displays a markedly higher crystalline volume fraction in comparison to the one prepared at $R=3$. Thus the increase of the hydrogen plasma treatment time induces an increase of the crystalline volume fraction. Furthermore, the crystalline fraction is higher for films deposited at lower values of T_{Si} ($T_{Si}=10$ s) and an intermediate value of R. Thinner is the stacking layer, shorter is the transition time from a-Si:H to μc-Si growth, and higher is the crystalline fraction. This could be explained by the lower energy necessary to arrange thinner a-Si:H layers.

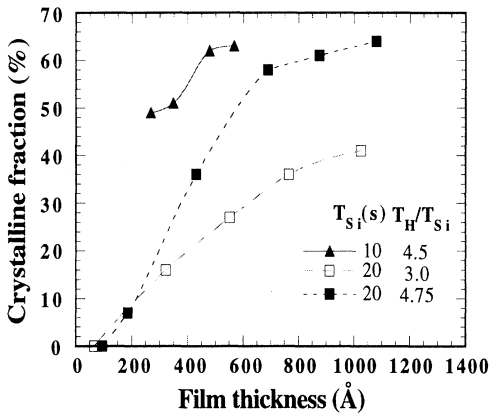

FIG. 10. Thickness dependence of the volume fraction of crystallites in the bulk of μc-Si films deposited by the layer-by-layer technique at two silicon deposition times ($T_{Si}=10$ and 20 s) and different values of the parameter $R=(T_H/T_{Si})$. Note that both the decrease of T_{Si} and the increase of T_H, for a given T_{Si}, result in a markedly higher crystalline volume fraction.

These results show that it is possible to control the volume fraction of crystallites in the film by varying the deposition and etching times in the layer-by-layer technique. They also show that it is possible to obtain thin layers (≈ 200 Å thick) with a high fraction of crystallites, and suggest that the incubation thickness can be reduced by reducing T_{Si}.

C. Microcrystalline silicon growth model

The results of this *in situ* ellipsometry study bring additional elements to the current models developed to explain the deposition of μc-Si films at low temperature by plasma-enhanced chemical-vapor deposition techniques. Let us discuss our results in the framework of these models.

(1) The partial equilibrium model[27] describes the deposition of μc-Si as the result of an equilibrium between deposition from SiH_x radicals and etching by atomic hydrogen. Indeed, we observe that the transition occurs when substantial etching ($\approx 30\%$) of the a-Si:H occurs during the hydrogen plasma exposure. However, it seems difficult within this model to explain the formation of μc-Si in 85-Å-thick films. The deposition of μc-Si by alternating more than ten atomic layers cannot be considered as a fast exchange between the surface of the solid and the plasma. Moreover, this model fails to explain the evolution of the surface composition, which should remain constant under equilibrium conditions, and the increase of the crystalline fraction in the bulk (Fig. 9). Therefore even though it may be reasonable to apply the partial chemical equilibrium model under steady-state conditions, this model does not explain neither the nucleation nor the evolution of the composition in μc-Si films.

(2) In the case of the selective etching model[28,29] the growth of μc-Si is explained by the fact that hydrogen selectively removes the amorphous phase. As an example, Fig. 11 clearly demonstrates the selective etching of a-Si:H. Figure 11 (left) shows an a-Si:H sample which was exposed after its growth to 160-mJ/cm^2 pulses from an XeCl laser at a repetition rate of 1 Hz.[12] As a consequence the central part of the sample was crystallized, while the sides remained amorphous. A sample deposited under the same conditions was exposed to a hydrogen plasma. As shown in the right side of Fig. 11, the entire amorphous part was etched by the hydrogen plasma but the crystalline area remained on the glass substrate.

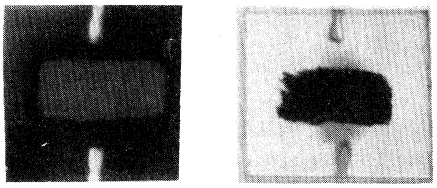

FIG. 11. Picture of two silicon films deposited on 1×1-in.^{2} glass substrate, giving experimental evidence of the selective etching. On the left side, an a-Si:H film was exposed to an excimer laser pulse which induced the crystallization of the central part of the sample. A similar film (right) was exposed to a hydrogen plasma under the conditions used in the layer-by-layer deposition. The hydrogen plasma completely removed the amorphous part.

While there is no doubt about the involvement of selective etching in the deposition of μc-Si films, its importance has to be carefully considered. Indeed, selective etching can be used to explain the increase of the crystalline fraction on the surface (Fig. 9) but it can hardly explain the simultaneous decrease of the void fraction. Moreover, as in the partial equilibrium model, the long-term evolution of the bulk composition, and the fact that crystallization takes place down to the interface with the glass substrate, cannot be explained.

(3) In the case of the hydrogen coverage model one assumes that the film structure is determined by the diffusion length of the film precursors.[20] At a high-H_2 dilution ratio, the hydrogen coverage factor increases. Consequently, the diffusion length of the precursors increases, resulting in μc-Si formation. As in the previous models, only the processes taking place on the surface of the growing sample are considered to explain the deposition of μc-Si films. Therefore, this model has the same limitations as the partial equilibrium and selective etching models.

(4) In the chemical annealing model, H atoms from the gas phase soak into the growth zone and react with SiH bonds. These chemical reactions are exothermic and the released energy induces an increase of the effective temperature of the film surface (chemical annealing), favoring the formation of μc-Si.[22,30] We point out that so far the chemical annealing has been applied to a relatively thin growth zone, just below the film growing surface, while our results indicate that the evolution of the bulk composition takes place down to some hundreds of Å. Moreover, the exposure of an a-Si:H film to a hydrogen plasma does not produce its crystallization but an increase of its porosity and surface roughness.[21] Both deposition and etching are necessary to the growth of μc-Si. Finally, the chemical annealing model does not explain the long term evolution of both the surface and bulk compositions.

To fully account for the deposition of μc-Si film a model should consider both the nucleation and growth of the crystalline phase. As far as the nucleation of the crystallites, we observe that they appear when a highly porous a-Si:H phase has been formed by the hydrogen plasma treatment. Indeed, a high degree of porosity seems to be a good way to release the strain in the dense a-Si:H film. Moreover, it has been reported that the hydrogen content of the films increases as the transition from a-Si:H to μc-Si deposition is approached.[31] Therefore, a highly porous and hydrogen-rich layer seems to be a necessary condition for the nucleation of the crystallites. The nucleation of the crystallites within this layer can be attributed either to a chemical annealing process or just to the reconstruction of the silicon network by atomic hydrogen. Once the nucleation of the crystalline phase has started, the long term evolution of the film properties can be described by a combination of the selective etching and the rearrangement of the bulk promoted by the diffusion of atomic hydrogen. While it seems reasonable to apply the chemical annealing model to a relatively thin growth zone, the evolution of the bulk composition in a depth higher than 600 Å can be explained by the diffusion of hydrogen which promotes the breaking of weak Si-Si bonds and the formation of the crystalline phase.

IV. SUMMARY AND CONCLUSION

The results of an *in situ* spectroscopic ellipsometry analysis of the evolution of the composition of a-Si:H and μc-Si films prepared on glass substrates at 250 °C by alternating a-Si:H deposition and hydrogen plasma treatment can be summarized as follows.

(1) The ratio $R=(T_H/T_{Si})$ is the principal parameter which determines the nature of the deposited material. The etching of the deposited film by the hydrogen plasma is directly evidenced by the real-time ellipsometry measurements.

(2) Layer-by-layer deposition is not well adapted to the deposition of dense a-Si:H, specially under the critical conditions corresponding to the boundary between a-Si:H and μc-Si. a-Si:H films deposited by LBL are more porous and rough, and have a lower dark conductivity than device quality a-Si:H.

(3) The layer-by-layer technique seems a promising technique for the deposition of μc-Si because it makes possible the control of the incubation time and the volume fraction of crystallites by a proper choice of T_H and T_{Si}.

(4) The growth of μc-Si films can be explained by combining, on the one hand, the selective etching which accounts for the evolution of the fraction of crystallites on the film surface, and, on the other hand, the diffusion of hydrogen which explains the development of the crystallites in the bulk.

In conclusion, our results show that the formation of a highly porous phase is a crucial step in the nucleation of μc-Si and that both selective etching of the disordered material on the surface and the atomic hydrogen diffusion in the bulk (few tens of nm) have to be considered in order to explain the nucleation and growth mechanisms of microcrystalline silicon films.

*Present address: AT&T Bell Laboratories, Murray Hill, 600 Mountain Avenue, NJ 07974.
†Author to whom all correspondence should be sent: Phone: 33-1-69-33 32 07. Fax: 33-1 69 33 30 06. Electronic address: roca@poly.polytechnique.fr

[1]J. Kanicki, *Amorphous and Microcrystalline Semiconductors Devices: Optoelectronic Devices* (Artech, London, 1991).
[2]H. Richter and L. Ley, J. Phys. (France) IV **43**, C1-247 (1982).
[3]R. W. Collins and B. Y. Yang, J. Vac. Sci. Technol. B **7**, 1155 (1989).
[4]M. Fang and B. Drévillon, J. Appl. Phys. **70**, 4894 (1991).
[5]S. Boultadakis, S. Logotheditis, S. Ves, and J. Kircher, J. Appl. Phys. **73**, 914 (1993).
[6]A. Asano, Appl. Phys. Lett. **56**, 533 (1990).
[7]N. Layadi, P. Roca i Cabarrocas, B. Drévillon, and I. Solomon, in *Proceedings of the 12th European Photovoltaic Solar Energy Conference, Amsterdam, 1994,* edited by R. Hill, W. Palz, and P. Helm (H.S. Stephens & Associaes, Bedford, UK, 1994).
[8]M. Otobe and S. Oda, Jpn. J. Appl. Phys. **31**, 1948 (1992).
[9]P. Roca i Cabarrocas, N. Layadi, T. Heitz, B. Drévillon, and I. Solomon, Appl. Phys. Lett. (to be published).
[10]R. W. Collins, Appl. Phys. Lett. **48**, 843 (1986).
[11]S. Kumar, B. Drévillon, and C. Godet, J. Appl. Phys. **60**, 1542 (1986).
[12]N. Layadi, P. Roca i Cabarrocas, J. Huc, J. Y. Parey, and B. Drévillon, Solid State Phenom. **37 & 38**, 281 (1994).
[13]B. Drévillon, J. Y. Parey, M. Stchakovsky, R. Benferhat, Y. Josserand, and B. Schlayen, SPIE Symp. Proc. **1188**, 174 (1990).
[14]R. M. A. Azzam and N. M. Bashara, *Ellipsometry and Polarized Light* (North-Holland, Amsterdam, 1977).
[15]G. E. Jellison, Jr., M. F. Chisholm, and S. M. Gorbatkin, Appl. Phys. Lett. **62**, 3348 (1993).
[16]D. E. Aspnes and A. A. Studna, Phys. Rev. B **27**, 985 (1983).
[17]D. A. G. Bruggeman, Ann. Phys. (Leipzig) **24**, 636 (1935).
[18]H. V. Nguyen and R. W. Collins, Phys. Rev. B **47**, 1911 (1993).
[19]M. J. Dignam and J. E. Fedyck, Appl. Spectrosc. Rev. **14**, 249 (1978).
[20]K. Nomoto, Y. Urano, J. L. Guizot, G. Ganguly, and A. Matsuda, Jpn. J. Appl. Phys. **29**, L1372 (1990).
[21]C. Godet and B. Drévillon, J. Vac. Sci. Technol. A **6**, 2482 (1988).
[22]H. Shirai, J. Hanna, and I. Shimizu, Jpn. J. Appl. Phys. **30**, L679 (1991).
[23]N. Blayo and B. Drévillon, Appl. Phys. Lett. **57**, 51 (1990).
[24]S. Aljishi, S. Jin, M. Stutzmann, and L. Ley, in *Materials Issues in Microcrystalline Semiconductors,* edited by P. M. Fauchet, K. Tanaka, and C. C. Tsia, MRS Symposia Proceedings No. 164 (Materials Research Society, Pittsburgh, 1990), p. 51.
[25]Y. H. Yang, M. Katiyar, J. R. Abelson, and N. Maley, in *Amorphous Silicon Technology—1993,* edited by E. A. Schiff, M. J. Thompson, A. Madan, R. Tanaka, and P. G. LeComber, MRS Symposia Proceedings No. 297 (Materials Research Society, Pittsburgh, 1993), p. 25.
[26]H. M. Branz, S. E. Asher, and B. P. Nelson, Phys. Rev. B **47**, 7061 (1993).
[27]S. Veprek, in *Materials Issues in Microcrystalline Semiconductors* (Ref. 24), p. 39.
[28]C. C. Tsia, G. B. Anderson, R. Thompson, and W. Wecker, J. Non-Cryst. Solids **114**, 151 (1989).
[29]I. Solomon, B. Drévillon, H. Shirai, and N. Layadi, J. Non-Cryst. Solids **164 & 166**, 989 (1993).
[30]J. Perrin, J. Non-Cryst. Solids **137, & 138**, 639 (1991).
[31]J. Jang, S. O. Koh, T. G. Kim, and S. C. Kim, Appl. Phys. Lett. **60**, 2874 (1992).

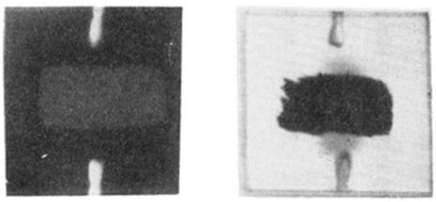

FIG. 11. Picture of two silicon films deposited on 1×1-in.^{2} glass substrate, giving experimental evidence of the selective etching. On the left side, an *a*-Si:H film was exposed to an excimer laser pulse which induced the crystallization of the central part of the sample. A similar film (right) was exposed to a hydrogen plasma under the conditions used in the layer-by-layer deposition. The hydrogen plasma completely removed the amorphous part.